Composites Part B 154 (2018) 439–448

Doi: 10.1016/j.compositesb.2018.08.096

Towards "green" viscoelastically prestressed composites: Cellulose fibre reinforcement.

Yang Qin, Kevin S. Fancey*

GW Gray Centre for Advanced Materials,

School of Engineering & Computer Science

University of Hull, HU6 7RX, UK

Abstract

With growing concerns over environmental issues, fibre reinforced composites based on renewable, biodegradable low-cost cellulosic/cellulose fibres increasingly attract interest. This paper reports on the first study to produce viscoelastically prestressed polymeric matrix composites (VPPMCs) using regenerated cellulose/viscose continuous fibres. The aim was to demonstrate that this prestressing technique could improve the mechanical properties of a cellulose fibre reinforced composite without the need to increase section mass or thickness. By investigating the viscoelastic properties of cellulose yarn, a suitable load was applied to subject the fibres to tensile creep. The load was then released and the loose yarns were moulded into a polyester resin matrix. Following matrix solidification, the viscoelastically recovering fibres imparted compressive stresses to the matrix. The mechanical properties of these cellulose fibre VPPMCs were investigated by tensile, three-point flexural and Charpy impact tests. Under the creep conditions investigated, the VPPMC samples demonstrated up to 20% increase in tensile strength and modulus and a comparable improvement in flexural properties, compared with control (unstressed) counterparts. Nevertheless, the prestress effect reduced impact toughness by ~30%, by impeding matrix crack formation and promoting fibre fracture. Based on findings from this paper, all-green VPPMCs may be achieved in the future by considering potentially suitable green resins.

Keywords: A. Polymer-matrix composites (PMCs); B. Residual/internal stress; D. Mechanical testing; Viscoelasticity.

* Corresponding author. Tel.: + 44 1482 465071.
E-mail address: k.s.fancey@hull.ac.uk (K.S. Fancey).

©2018, Elsevier. This manuscript version is made available under the CC-BY-NC-ND 4.0 license http://creativecommons.org/licenses/by-nc-nd/4.0/

1. Introduction

Despite the widespread use of conventional glass and carbon fibre reinforcements in polymeric composites, there has been increasing awareness of their environmental and sustainability issues; i.e. the carbon dioxide emissions and energy consumption during their manufacture as well as the potential tonnage of non-degradable waste at the end of product life. [1-6]. Therefore, interest in "green" fibre reinforcement as a substitute for glass or carbon fibres in various applications is increasing rapidly.

Renewable and biodegradable cellulosic or regenerated cellulose fibres are of prominent importance in this regard. In addition, these fibres are readily available, cost-effective, non-toxic and have low densities [3, 5, 7-11]. Darshil et al. [12] found that by substituting E-glass fibres with flax fibres in a polyester matrix, a 3.5 m composite rotor blade (suitable for an 11 kW turbine) showed a 10% decrease in structural weight whilst maintaining operational integrity requirements. Another study [13] demonstrated that retrofitted flax fibre-polymer composite strips, for the seismic strengthening of reinforced concrete, could dissipate greater energy than (more conventional) carbon fibre equivalents. Composites based on cellulosic fibres such as sisal, eucalyptus, flax, kenaf, bamboo, hemp, abaca and wheat straw have already been adopted in producing roofing tiles, and automotive products, i.e. door trim panels, seat foams, engine and transmission enclosures [7, 14-16]. Nevertheless, one disadvantage of natural cellulosic fibres is their variation in fibre characteristics, which can result in composites with unpredictable mechanical properties [17]. Thus man-made/regenerated cellulose fibres such as viscose, lyocell and rayon with relatively stable characteristics have attracted significant attention as fibre reinforcements [18-26]. Fink et al. [22] demonstrated that man-made cellulose fibres can considerably enhance thermoplastic polymers (polypropylene, polyethylene) in terms of strength, stiffness and impact resistance. Moreover, a Charpy impact study of PLA (polylactic acid) reinforced with Cordenka rayon fibre showed that composite impact strength could reach to 72 kJ/m^2, suggesting potential applications in the automotive and electronic industries, as a substitute for traditional composite materials [23].

Despite these positive aspects, the mechanical properties of cellulosic/cellulose fibre reinforced composites (CFRCs) are poor compared with conventional carbon/glass fibre composites. Therefore investigations into improving the mechanical properties of CFRCs are of major importance for wider practical applications. It is believed that the poor fibre-matrix interfacial adhesion of CFRCs can limit their mechanical properties, due to incompatibility between the hydrophobic polymeric matrix and hydrophilic cellulosic/cellulose fibre [4-7, 11, 27]. Many researchers have focused on fibre surface treatments (coupling agent, alkali, ultraviolet, cold plasma, etc.) and achieved considerable mechanical improvements [3, 4, 6, 7, 9]. Nevertheless, these surface treatment methods can have environmental issues, and require expensive equipment [28, 29].Thus investigation into a relatively simple, "green", low-cost method for mechanical improvement is required.

The concept of viscoelastically prestressed polymeric matrix composites (VPPMCs) was first published in 2000 [30]. By utilising the viscoelastic characteristics of specific fibre reinforcements, such as nylon 6,6 and ultra-high molecular weight polyethylene (UHMWPE) fibres, VPPMCs could produce significant improvements in mechanical properties compared with their unstressed control counterparts, without the need to increase section size or weight. Nylon 6,6 fibre-based VPPMCs have shown ~15% increase in tensile strength and 25–50% improvements in impact strength and flexural stiffness [31-36]. In addition, accelerated ageing has demonstrated no degradation in VPPMC impact strength for at least 25 years even when exposed to 50 °C ambient temperature [36]. For VPPMCs with UHMWPE fibres, 20–40% increases in flexural modulus and Charpy impact strength have also been demonstrated [37, 38]. To produce VPPMCs, fibre reinforcements are stretched under a fixed stress (creep) for a predetermined time period; the tensile stress is then released before moulding the prestressed fibres into a resin matrix. The prestressed fibres will undergo viscoelastic recovery, so that following matrix curing, compressive stresses are generated within the matrix (counterbalanced by fibre tension), leading to improved mechanical properties. One of the key advantages of VPPMCs is that unlike conventional elastically prestressed polymeric matrix composites (EPPMCs), the fibre stretching and moulding processes are

©2018, Elsevier. This manuscript version is made available under the CC-BY-NC-ND 4.0 license http://creativecommons.org/licenses/by-nc-nd/4.0/

decoupled. Thus stretching equipment can be relatively simple and the unconstrained fibres can be used in producing composite structures with complex geometries [39].

Some studies have demonstrated the time-dependent viscoelastic behaviour of hemp, bamboo and regenerated cellulose fibres such as rayon, over short-time periods (minutes to hours) [40-44]. Moreover, the flexural behaviour of VPPMCs based on prestressed bamboo slivers have shown a 28% increase in flexural toughness compared with unstressed counterparts [45]. Nevertheless the use of bamboo slivers can clearly present challenges in stretching and moulding, due to their large size and discontinuous nature.

This paper reports on the first study to evaluate the use of green continuous fibres for generating the prestress within a VPPMC. Here, the long-term viscoelastic recovery characteristics of regenerated cellulose fibre (viscose) was investigated and the resulting VPPMCs were studied under tensile, flexural and Charpy impact test conditions.

2. Background

2.1. Viscoelastic behaviour

A viscoelastic material can store deformation energy under tensile creep. After releasing the creep load, though stored energy is released initially through instantaneous elastic recovery, a substantial proportion of energy can be released progressively during long-term viscoelastic recovery. To investigate the viscoelastic behaviour of regenerated cellulose fibre, the strain-time assessment of creep and recovery processes has been employed in this study, being a relatively convenient method.

Fig. 1 represents the general strain-time creep and recovery characteristics of a viscoelastic material. Previous findings have demonstrated that polymeric creep and recovery can be represented by Weibull or Kohlrausch–Williams–Watts functions [46]. The time dependent creep strain $\varepsilon_{ctot}(t)$ is given by:

$$\varepsilon_{ctot}(t) = \varepsilon_i + \varepsilon_c \left[1 - \exp\left(-\left(\frac{t}{\eta_c}\right)^{\beta_c}\right)\right] \quad (1)$$

where ε_i is the instantaneous elastic strain; ε_c represents the time-dependent component in which η_c and β_c are the characteristic life and shape parameters respectively.

After releasing the tensile creep stress and following the instantaneous recovery strain ε_e, the (time dependent) viscoelastic recovery strain $\varepsilon_{rvis}(t)$ can be expressed as:

$$\varepsilon_{rvis}(t) = \varepsilon_r \left[\exp\left(-\left(\frac{t}{\eta_r}\right)^{\beta_r}\right)\right] + \varepsilon_f \quad (2)$$

where the ε_r function shows the recovery strain with parameters η_r and β_r being the associated characteristic life and shape parameters. Permanent strain resulting from viscous flow effects is represented by ε_f.

If viscoelastic recovery occurs at a fixed strain, a stress will be generated as the fibre attempts contraction, as shown in Fig. 2 [47]. This represents the principle of imparting compressive stresses within a VPPMC, following matrix solidification. The viscoelastic recovery stress, measured under a fixed strain, would not be identical to the stress locked within a VPPMC however, since the former represents ideal matrix conditions (i.e. no matrix deformation). Nevertheless, the result provides an indication of stress magnitude. The time-dependent recovery stress, $\sigma(t)$, i.e. recovery force over fibre cross sectional area, can be represented as [47]:

©2018, Elsevier. This manuscript version is made available under the CC-BY-NC-ND 4.0 license http://creativecommons.org/licenses/by-nc-nd/4.0/

$$\sigma(t) = \sigma_v \left[\exp\left(-\left(\frac{\Delta t}{\eta} \right)^{\beta} \right) - \exp\left(-\left(\frac{t}{\eta} \right)^{\beta} \right) \right] \quad (3)$$

where η and β are the associated Weibull parameters within the σ_v function, Δt is the time interval between releasing the creep stress and initiation of the recovery stress (Fig. 2). Details of the measurement process are given in Section 3.2.

Previous investigations with nylon 6,6 and UHMWPE fibres demonstrated that annealed fibres exhibit significantly higher creep and recovery strain than non-annealed (as-received) fibres under identical conditions [37, 48, 49]. Thus in this paper, the influence of annealing treatment is studied.

2.2. Three-point flexural testing

The flexural properties could be investigated through evaluating the flexural modulus E_f and associated stress σ_f, under three-point bending conditions. According to the ASTM D790 standard [50], E_f is represented as:

$$E_f = L^3 m / 4bd^3 \quad (4)$$

where L is the support span; b and d are the sample width and depth respectively. The slope of the tangent to the initial linear region of the load-deflection curve is represented by m. The associated stress, σ_f, is given as:

$$\sigma_f = 3PL / 2bd^2 \quad (5)$$

where P is the load at a given point on the load-deflection curve.

The flexural strain, r, is defined as:

$$r = 6dD / L^2 \quad (6)$$

where D represents the midspan deflection. The standard is not applicable beyond r = 5%.

3. Experimental procedures

3.1. Materials

The fibre reinforcement was regenerated cellulose (viscose) yarn of 600 denier consisting of 120 fibres; the cross-sectional area of each fibre was ~370 μm^2. The yarn was supplied by Xinxiang Sunshining Textiles Co. Ltd., Henan, China. The matrix material was Reichhold Polylite 32032, a clear polyester casting resin supplied by MB Fibreglass, UK, mixed with 2% MEKP catalyst.

©2018, Elsevier. This manuscript version is made available under the CC-BY-NC-ND 4.0 license http://creativecommons.org/licenses/by-nc-nd/4.0/

3.2. Fibre creep, recovery and recovery stress investigations

Viscoelastic characteristics of the cellulose yarn were investigated to determine appropriate loading conditions for prestress generation. Previous VPPMC studies with nylon 6,6 and UHMWE fibres [37, 48] have shown that annealing the yarn prior to stretching improves viscoelastic properties. Based on an investigation by Dadashian et al [51], cellulose yarns were annealed at 120 °C for 0.5 h in a fan-assisted oven; only minor changes in fibre strength and breaking extension were observed from this annealing condition in Ref. [51]. For the creep-recovery strain measurements, a calibrated small stretching rig with digital cursor (± 0.01 mm precision) was used as in previous studies [35, 37, 48]. The cellulose yarn, with 250 mm marked gauge length, was suspended on the loading rig through upper and lower bobbins, typically 300-400 mm apart, the lower bobbin being mounted on a counterbalanced platform for weights to be applied. A 24 h creep duration was used, during which the strain was recorded and, following release of the tensile stress, recovery strain was also recorded in situ.

For recovery stress measurement, a bespoke force measurement rig with force sensor was employed for this purpose, as previously described [47]. Following the 24 h creep of cellulose yarn on the stretching rig, the tensile stress was released and the loose cellulose yarn (with bobbins) was transferred to the force measurement rig as quickly as possible. After a short period of time Δt (Fig. 2), the initially loose yarn became progressively tightened due to viscoelastic recovery. The resulting recovery stress was monitored through the force sensor at fixed strain. All measurements were performed under ambient conditions of 20-21 °C and 35–42% RH.

From preliminary trials, a tensile stress value of 190 MPa was selected for the 24 h creep process. Viscoelastic recovery strain and stress values were measured up to 1000 h. For repeatability, measurements were made on two separate yarn samples, for both annealed and non-annealed cases. Eqs. (1)–(3) were applied to fit creep-recovery strain and recovery stress results from the yarns by curve fitting with *Matlab® R2015a* software.

3.3. Sample production

Sample production methods were similar to those used for nylon 6,6 and UHMWPE fibre composites [30, 33-36, 48, 49, 52]. Two identical cellulose yarns (one "test", one "control") were annealed simultaneously as described in Section 3.2. The test yarn was then stretched under 190 MPa for 24 h by a large stretching rig which, for composite production, could subject a greater quantity of yarn to creep as previously described [53]. The control yarn was placed in close proximity to the rig, for exposure to the same environmental conditions (20–21 °C, 35–45% RH) during the stretching process of test yarns. Following stretching, both yarns were cut and folded into suitable lengths before casting. In contrast with nylon 6,6 and UHMWPE yarns in previous studies [30-38, 48, 49, 52, 54, 55], the cellulose yarns were not brushed out to separate the fibres, due to the high risk of fibre damage.

For composite sample production, two sets of moulds were used, one set to produce samples for tensile testing, the other for flexural and impact testing. Each set consisted of two identical moulds, to ensure the simultaneous production of test (prestressed) and control (unstressed) samples. For tensile testing samples, closed moulds, based on the "leaky mould" concept from work by Ladizesky and Ward [56] were used. The depth of the polished channel (10 mm wide) within each leaky mould was adjusted to produce samples of 1 mm thickness using spacers, as previously described [31]. For flexural and impact samples, two aluminium open-casting moulds, each with a polished channel (10 mm wide, 3 mm deep) were used, as in previous work [30, 32-39, 48, 52, 57]. Demoulding of composite strips from both sets of moulds was conducted ~2 h after casting; both test and control strips were then cut into required lengths to obtain sample batches. For flexural and impact testing, each batch consisted of 5 test and 5 control samples; while for tensile testing, 2 test and 2 control samples formed a batch. Prior to mechanical testing, all samples were placed under steel weights in ambient conditions (19–21 °C) for ~336 h (2 weeks), to

©2018, Elsevier. This manuscript version is made available under the CC-BY-NC-ND 4.0 license http://creativecommons.org/licenses/by-nc-nd/4.0/

prevent possible distortion from residual stresses. Fibre volume fractions (V_f) were ~9.4% and ~6.7% for flexural and impact tests respectively; three V_f values, i.e. 11%, 21% and 32 % were investigated for tensile testing. Beam sample geometry for tensile testing was 200 × 10 × 1 mm, based on CRAG [58]; for both flexural and impact testing, sample dimensions were 80 × 10 × 3.2 mm according to ASTM D790 and EN ISO 179 standards [50, 59]. In addition, for tensile testing, high impact polystyrene tabs (25 mm long, 1.9 mm thick) were glued with polyester resin (used for the matrix) at both ends of each sample. This was in accordance with CRAG [58], in order to minimise stress concentration effects in the vicinity of the clamping regions during testing.

3.4. Cellulose fibre tensile tests and microscopy investigations

To investigate whether the stretching process would affect the tensile mechanical properties of the cellulose fibre, a TA Instruments Q800 Dynamic Mechanical Analyser (DMA) in force-controlled tension mode was employed for fibre tensile testing as in previous studies with nylon 6,6 fibre [31]. Six (prestressed) test fibres and six (unstressed) control fibres, all being annealed before stretching, were selected randomly with a 10 mm testing gauge length. The preload and ramp force rate were set at 0.0001 N and 0.25 N/min respectively [31]. These tensile tests were performed at ~336 h (2 weeks) after the stretching process, at 20 °C. Tensile modulus, strength and strain-to-failure (STF) were recorded.

Scanning electron microscopy (SEM) was used to investigate possible changes in the topography of cellulose fibres after the stretching process and optical microscopy (OM) was employed to study the fibre spatial distribution from cross sections for all composite sample types.

3.5. Mechanical testing and post fracture analysis

Tensile, three-point flexural and Charpy impact tests were applied to evaluate the mechanical characteristics of the test and control composite samples. Tensile and flexural tests were both performed on a Lloyds EZ50 universal materials testing machine, using pull-to-break and bend-to-rupture modes respectively. For tensile testing, the tensile modulus, strength and STF were provided by stress-strain curves at a loading rate of 5 mm/min [31]. Three-point flexural tests were based on ASTM D790 [50]; the test span and indenter motion rate were set at 52 mm (span-to-depth ratio of ~16) and 1.41 mm/min. Flexural tests were terminated after reaching the 5% strain limit (midspan deflection of 7.04 mm from Eq. (6)). Flexural properties were compared through stress-strain curves calculated from Eq. (4) and (5). A Ceast Resil 25 Charpy machine with a 7.5 J hammer and velocity of 3.8 m/s was employed for Charpy impact testing, according to EN ISO 179 [59]. A 24 mm test span was applied to be consistent with previous work [30, 33-36, 38, 48, 49, 52, 57].

As observed in studies with nylon 6,6 and UHMWPE fibres [30, 34, 37, 48], sample cross sections indicated that most of the cellulose fibres were concentrated towards the bottom face of the open-casting mould. Thus all test and control samples for flexural and Charpy impact tests were positioned on machines with the cellulose fibre-rich side facing away from the indenter or hammer to maximise composite performance. All tests were conducted at room temperature (20-22 °C). Following Charpy impact tests, fractured samples were analysed by SEM.

4. Results and discussion

4.1. Cellulose fibre creep, recovery and recovery stress

Creep, recovery strains and recovery stress for both annealed and non-annealed cellulose fibres with the curve fittings are plotted in Figs. 3–5. In contrast with the major differences in viscoelastic characteristics between annealed and non-annealed nylon 6,6 or UHMWPE fibres [37, 48, 49], the

©2018, Elsevier. This manuscript version is made available under the CC-BY-NC-ND 4.0 license http://creativecommons.org/licenses/by-nc-nd/4.0/

cellulose yarns show only minor changes from annealing. It is clear that the curves from both annealed and non-annealed cellulose fibres in Fig. 4 show long-term viscoelastic characteristics and importantly, the ε_f values are insignificant, indicating negligible (unwanted) permanent strain from viscous flow. Moreover, the recovery stress, as observed in Fig. 5, progressively increases; the stress outputs are predicted to be ~51 MPa and ~61 MPa for non-annealed and annealed cellulose fibres respectively as $t \rightarrow \infty$. These values are considerably greater than the value (15.4 MPa) for nylon 6,6 fibre [39]. Thus there is sufficient evidence to support the feasibility of cellulose fibre-based VPPMC production. Based on the observed scatter and correlation coefficient (r) from the curve fittings however, the non-annealed cellulose yarns show greater variability, especially in recovery and recovery stress (Figs 4 and 5). It is speculated that this larger variation is caused by the non-uniform stress history within the regenerated cellulose fibre, possibly induced by extrusion and drawing during manufacture [60]. The annealing treatment is expected to remove the previous stress history [31], leading to more consistent viscoelastic behaviour, as observed in Figs. 3–5. Consequently, all cellulose fibres used in composite sample production and fibre tensile tests in this study were annealed.

4.2. Composite photographic assessment

Fig. 6 shows typical cellulose yarn spatial distributions by OM from cross sections for all three types of sample (for tensile samples, only the 21% V_f samples were studied). The distribution of yarns are visible, each yarn consisting of many individual fibres. For tensile samples (produced by the leaky mould technique), the cellulose yarns show the most uniform distributions. For open moulded flexural and impact samples, the yarns have a tendency to concentrate closer to the bottom of the moulds as reported in Section 3.5. There appear to be no significant differences in yarn spatial distributions between test and control for all sample types. Nevertheless, yarns can be seen to have oval profiles in the control samples, as opposed to a circular shape in the test samples. The circular profile must arise from lateral compaction effects within the yarns due to the stretching process.

4.3. Cellulose fibre assessment

Fig. 7 shows SEM micrographs of test (prestressed) and control cellulose fibres (both being annealed). There appear to be no visible changes in the fibre topography following the stretching process.

Results from DMA cellulose fibre tensile tests are summarised in Table.1. The tensile modulus was measured in the (assumed) elastic strain region from 0.3–1.0% strain, to compensate for the "toe region" in the initial stage of a typical stress-strain curve. The mean values for all three tensile parameters appear to show no statistical difference between test and control fibres, based on two-tailed hypothesis testing (at 5% significance level).

Table 1

Summary of single cellulose fibre DMA tensile test results (6 test and 6 control); SE represents the standard error of the mean.

	Mean Tensile Strength ± SE, (MPa)	Mean Tensile Modulus ± SE, (GPa)	Mean Strain-to-Failure ± SE, (%)
Test	342.33 ± 10.80	9.41 ± 0.41	16.22 ± 4.79
Control	350.01 ± 16.98	8.83 ± 0.38	17.85 ± 3.02

©2018, Elsevier. This manuscript version is made available under the CC-BY-NC-ND 4.0 license http://creativecommons.org/licenses/by-nc-nd/4.0/

The above findings suggest that the 190 MPa 24 h stretching process has no significant influence on the cellulose fibre topography or tensile properties. This increases confidence that any observed differences in VPPMC performance over control counterparts can be attributed to viscoelastically generated prestress effects.

4.4. Tensile tests

Fig. 8 shows typical stress-strain curves for both test and control composite samples at three V_f values (11%, 21% and 32%). The tensile modulus was determined from the observed linear region from 0–0.33%. Although tabs were employed at both ends of each sample to reduce unwanted stress concentration effects, some samples still fractured near the clamps of the universal testing machine. Thus, to reduce experimental uncertainty, only those samples that fractured near their centres were utilised for analysis. Thus sample numbers were 9 test and 9 control, 8 test and 10 control, 7 test and 5 control for V_f values of 11%, 21% and 32% respectively. Tensile strength, modulus and STF results are summarised in Figs 9–11 as a function of V_f.

As expected, Figs 9 and 10 show that tensile strength and modulus both increase with V_f. For all three V_f values, the VPPMCs show increased strength and modulus compared with control samples. Three mechanisms can be attributed to the improvement and are summarised here. First, during tensile testing, compressive stresses within the VPPMCs directly resist the tensile load, leading to improved tensile properties. Second, it is suggested by Motahhari and Cameron [61] that the taut fibres could respond instantaneously and more collectively to external stresses in conventional EPPMCs. Although fibre waviness in our VPPMC samples still exists, it has been suggested that this mechanism may still be effective in improving tensile properties [31]. Finally, the fracture of a fibre within a unidirectional FRC can result in a stress wave propagating outwards, causing dynamic overstress to facilitate the fracture of neighbouring fibres [62]. It is proposed that this effect may be alleviated by the induced compressive stresses, therefore strengthening the VPPMCs [31].

Figs. 9 and 10 also indicate an optimum V_f occurs close to 21%, where 19.6% and 19.0% increases are observed for tensile strength and modulus respectively. As previously reported for nylon 6,6 fibre VPPMCs [31], this optimum V_f is believed to be an outcome from competing mechanisms between fibre reinforcement and the matrix. Here, too few fibres reduce the magnitude of compressive stresses within the sample, but too many fibres would reduce matrix cross sectional area, thereby reducing the compressive stress effect. We also suggest that higher V_f values may hinder matrix permeation between fibres, further weakening compressive forces.

The STF for polyester resin is found to be 4.7% [63], which is ~1/3 that of the cellulose fibres (~17%) in Table 1. Therefore, this may explain the increased STF with V_f for both test and control samples, as can be seen in Fig. 11. The STF of VPPMCs show a 50-60% decrease compared with control counterparts, for all three V_f values in Fig. 11. It can be speculated that compressive stresses within the test samples could impede sample extension during tensile tests, i.e. a lower STF is observed. Also, in contrast with the taut fibres within the test samples, fibres within the control samples would not be expected to respond to external tensile stresses collectively [61], so that fibre fractures may proceed more progressively. This would contribute to greater sample displacement (higher STF) for control samples during the fibre fracture process [31].

4.5. Three-point flexural tests

Typical test and control stress-strain curves from the three-point flexural tests are shown in Fig. 12. To compensate for the toe region, the flexural modulus is measured in the linear region from 0.3–1.0% strain. It is clear that both test and control samples show ductile flexural behaviour, as samples neither

©2018, Elsevier. This manuscript version is made available under the CC-BY-NC-ND 4.0 license http://creativecommons.org/licenses/by-nc-nd/4.0/

yield nor break before the 5% strain limit according to the ASTM D790 standard [50]. The modulus and stress results from 8 batches (5 test and 5 control samples per batch) are summarised in Table 2. The relatively small standard errors within each batch and in the means from all batches demonstrate good repeatability. For all batches, test samples show increases in flexural modulus and stress (compared with control samples), of ~5% and ~15% respectively.

For some studies in which a more uniform fibre spatial distribution could be obtained through the sample thickness, improvements in flexural properties have been attributed to fibre tension (from prestress) resisting deflection from applied bending forces [32, 61]. In this study however, most of the fibres were concentrated in the composite tensile region under flexural testing. Therefore, the resulting compressive stresses within the tensile region of the test samples will shift the neutral axis downward towards the lower sample surface. This reduces the magnitude of flexural tensile stress in the test sample, i.e. improving flexural properties [32, 64]. Moreover, as discussed in Section 4.4, the taut fibres in the test samples could respond to external forces more collectively, leading to improved flexural properties [61].

Table 2

Three-point flexural results for 8 batches of samples (i.e. 40 test, 40 control); SE represents the standard error of the mean.

Batch Number	Flexural Modulus (GPa)		Increase (%)	Flexural Stress at 5% Strain Limit (MPa)		Increase (%)
	Test ± SE	Control ± SE		Test ± SE	Control ± SE	
1	2.27 ± 0.04	2.20 ± 0.02	3.10	87.66 ± 1.56	73.38 ± 0.31	19.46
2	2.24 ± 0.03	2.00 ± 0.05	11.77	80.48 ± 1.31	68.44 ± 0.96	17.60
3	2.15 ± 0.05	2.07 ± 0.06	3.81	81.26 ± 1.27	68.12 ± 2.27	19.29
4	2.20 ± 0.05	2.05 ± 0.02	7.48	82.15 ± 2.56	70.72 ± 0.73	16.17
5	2.13 ± 0.04	2.06 ± 0.03	3.29	76.27 ± 1.25	65.87 ± 0.76	15.78
6	2.08 ± 0.02	1.98 ± 0.04	4.97	78.24 ± 0.93	67.53 ± 1.03	15.85
7	1.90 ± 0.04	1.83 ± 0.04	3.63	71.77 ± 1.15	65.16 ± 1.13	10.15
8	2.21 ± 0.01	2.18 ± 0.04	1.39	87.60 ± 0.47	78.68 ± 0.94	11.35
Mean ± SE	2.15 ± 0.04	2.05 ± 0.04	4.93 ± 1.16	80.68 ± 1.91	69.74 ± 1.58	15.71 ± 1.20

4.6. Charpy impact tests and fracture mechanism studies

Table 3 shows Charpy impact testing results from 5 batches (5 test and 5 control samples per batch). In contrast with the improved tensile and flexural results above, the test samples absorb less energy than their control counterparts, by an average of 32.5%. The result clearly indicates that prestressing has a negative influence on the composite impact strength. Previous Charpy impact investigations on nylon 6,6 and UHMWPE fibre based VPPMCs have demonstrated ~40% and ~20% more energy absorption than their control counterparts respectively [33-36, 38]. The primary mechanism for this improvement was suggested to be shear stresses induced by fibre viscoelastic recovery, which could promote debonding at fibre-matrix or (within UHMWPE fibres) fibre skin/core interfaces, leading to greater energy absorption during the impact process.

Fracture characteristics from the cellulose composites and, for comparison, nylon 6,6 composites from previous testing are shown in Fig. 13. It is clear that both test and control cellulose composite samples fracture entirely into two separate pieces without the visible fibre-matrix debonding (lighter regions) observed in the nylon 6,6 composites. Also, in contrast with the nylon 6,6 composites, lateral cracks are observed on both cellulose samples, especially on the control sample. Fewer lateral cracks (resulting in less energy absorption) on the test sample is likely to result from the longitudinal compressive stresses within the matrix, which could impede the formation and propagation of these cracks.

©2018, Elsevier. This manuscript version is made available under the CC-BY-NC-ND 4.0 license http://creativecommons.org/licenses/by-nc-nd/4.0/

An additional explanation for reduced energy absorption by the test samples is proposed here. The STF of cellulose fibres (~17%) is ~50% of nylon 6,6 fibres (~30% [31]), suggesting more brittle characteristics for the cellulose fibres. Thus, it is suggested that, from the relatively high strain rate during impact, crack propagation is more likely to favour fibre fracture than alter its direction to spread along the fibre-matrix interface (debonding). The prestressed taut fibres in the test samples would exacerbate the situation, resulting in less energy absorption during the fibre fracture.

Table 3

Charpy impact results from 5 batches of samples (i.e. 25 test, 25 control); SE represents the standard error of the mean.

Batch Number	Mean Impact Energy (kJ/m^2)		Increase (%)
	Test ± SE	Control ± SE	
1	15.51 ± 0.87	26.96 ± 1.46	-42.46
2	20.79 ± 0.92	28.04 ± 1.52	-25.83
3	17.61 ± 0.71	24.26 ± 1.63	-27.38
4	17.29 ± 0.79	27.79 ± 0.96	-37.79
5	20.11 ± 0.48	28.37 ± 0.43	-29.10
Mean ± SE	18.26 ± 0.97	27.08 ± 0.74	-32.51 ± 3.24

Fig. 14 shows SEM micrographs of representative test and control samples at the fracture sections. Fracture mechanisms consisting of matrix cracking, fibre fracture and fibre pull-out can be observed on both samples without significant differences. Previous Charpy impact tests on nylon based composites demonstrated the "mushroom" effect (i.e. swelling) at fractured nylon fibre ends [53]. On the contrary, the ends of fractured cellulose fibres, in both test and control samples, are relatively flat (undeformed). This also indicates that cellulose fibres are less ductile, which would encourage fibre fracture, in contrast with the tougher nylon fibres. As discussed in Section 4.2, fibres in the test yarns undergo lateral compaction as a result of the stretching process (Fig. 6). Nevertheless, Fig. 14 shows that all fibres are well permeated by the matrix resin. Thus differences in compaction between the test and control cellulose yarns is believed to have no significant influence on composite properties. Moreover, fibres visible from pull-out show clean surfaces (i.e. no matrix material adhesion), which provides evidence of poor fibre-matrix interfacial bonding as observed in other cellulose fibre composite studies [21, 26]. Cellulose fibre VPPMCs utilising other matrix materials however, may differ in their fibre-matrix bonding characteristics, which could improve impact strength.

5. Conclusion

The viscoelastic behaviour of regenerated cellulose (viscose) yarns has been investigated. Tensile, three-point flexural and Charpy impact tests have been performed to compare the mechanical properties between cellulose fibre based VPPMCs and their unstressed (control) counterparts. The summarised findings are:

i. By employing an appropriate creep stress, the cellulose yarns demonstrated long-term viscoelastic characteristics under both recovery strain and stress conditions. In addition, annealing prior to stretching provided the cellulose yarns with more consistent viscoelastic behaviour, making them better suited to VPPMC production.
ii. In tensile tests, the tensile strength, modulus and STF increased with increasing V_f for both test and control samples. It was demonstrated that for all three V_f values (11%, 21%, 32%), test samples showed higher tensile strength and modulus than their control counterparts due to the

©2018, Elsevier. This manuscript version is made available under the CC-BY-NC-ND 4.0 license http://creativecommons.org/licenses/by-nc-nd/4.0/

counteracting effect from compressive stresses and a more collective response to external tensile forces. An optimum V_f close to 21% was indicated, where increases of ~20% were observed for both tensile strength and modulus. A 50-60% decrease in STF was observed for test samples at all three V_f values.

iii. Compared with control samples, the test samples showed ~5% and ~15% increases in flexural modulus and stress from three-point bending tests. The improvement may be attributed to the compressive stresses within a test sample, shifting the neutral axis towards the bottom of the sample, leading to reduced flexural tensile stress. In addition, the taut fibres in a test sample can be expected to respond more collectively to lateral forces.

iv. Prestressing showed a negative effect on the composite impact strength. The test samples demonstrated ~30% decrease in impact energy absorption compared with control samples. This is attributed to compressive stresses impeding the formation of (energy absorbing) cracks in a test sample matrix. Also, cellulose fibres have low ductility; thus it is suggested that fibre fracture is exacerbated within the taut, prestressed fibres in a test sample, in contrast with greater energy absorption from fibre-matrix debonding.

Our study has demonstrated improvements in both modulus and strength by applying the concept of viscoelastically prestress to CFRCs and future investigations into the fibre prestress treatment may enhance these improvements. Cellulose fibres, being renewable and biodegradable, open up opportunities for "green" VPPMC production, by substituting polyester resin with a green matrix material, such as PLA or vegetable oil-based epoxy. Moreover, as cellulose is one of the major components of most natural fibres, the improvement in mechanical properties, as demonstrated by our cellulose fibre-based VPPMCs, may lead to the prestressing technique being applied to a range of natural fibres. This could enhance the performance of various natural fibre composites that are already utilised within engineering applications.

Acknowledgements

Support from the Hull-China Scholarship Council agreement for one of the authors (YQ), is gratefully acknowledged. The authors would also like to thank Garry Robinson and Sue Taft from the School of Engineering & Computer Science for SEM and DMA technical support.

References

[1] Joshi SV, Drzal L, Mohanty A, Arora S. Are natural fiber composites environmentally superior to glass fiber reinforced composites? Compos Part A 2004;35(3):371-6.

[2] Pickering SJ. Recycling technologies for thermoset composite materials—current status. Compos Part A 2006;37(8):1206-15.

[3] Satyanarayana KG, Arizaga GG, Wypych F. Biodegradable composites based on lignocellulosic fibers—An overview. Prog Polym Sci 2009;34(9):982-1021.

[4] Faruk O, Bledzki AK, Fink H-P, Sain M. Biocomposites reinforced with natural fibers: 2000–2010. Prog Polym Sci 2012;37(11):1552-96.

[5] Jauhari N, Mishra R, Thakur H. Natural Fibre Reinforced Composite Laminates–A Review. Mater Today 2015;2(4-5):2868-77.

[6] Pickering KL, Efendy MA, Le TM. A review of recent developments in natural fibre composites and their mechanical performance. Compos Part A 2016;83:98-112.

[7] Bledzki A, Gassan J. Composites reinforced with cellulose based fibres. Prog Polym Sci 1999;24(2):221-74.

©2018, Elsevier. This manuscript version is made available under the CC-BY-NC-ND 4.0 license http://creativecommons.org/licenses/by-nc-nd/4.0/

[8] Klemm D, Heublein B, Fink HP, Bohn A. Cellulose: fascinating biopolymer and sustainable raw material. Angew Chem Int Edit 2005;44(22):3358-93.

[9] Li X, Tabil LG, Panigrahi S. Chemical treatments of natural fiber for use in natural fiber-reinforced composites: a review. J Polym Environ 2007;15(1):25-33.

[10] John MJ, Thomas S. Biofibres and biocomposites. Carbohyd Polym 2008;71(3):343-64.

[11] Gurunathan T, Mohanty S, Nayak SK. A review of the recent developments in biocomposites based on natural fibres and their application perspectives. Compos Part A 2015;77:1-25.

[12] Shah DU, Schubel PJ, Clifford MJ. Can flax replace E-glass in structural composites? A small wind turbine blade case study. Compos Part B 2013;52:172-81.

[13] Di Luccio G, Michel L, Ferrier E, Martinelli E. Seismic retrofitting of RC walls externally strengthened by flax-FRP strips. Compos Part B 2017;127:133-149.

[14] Cook D, Pama R, Weerasingle H. Coir fibre reinforced cement as a low cost roofing material. Build Environ 1978;13(3):193-8.

[15] Mehta G, Mohanty AK, Thayer K, Misra M, Drzal LT. Novel biocomposites sheet molding compounds for low cost housing panel applications. J Polym Environ 2005;13(2):169-75.

[16] Koronis G, Silva A, Fontul M. Green composites: a review of adequate materials for automotive applications. Compos Part B 2013;44(1):120-7.

[17] Yan L, Kasal B, Huang L. A review of recent research on the use of cellulosic fibres, their fibre fabric reinforced cementitious, geo-polymer and polymer composites in civil engineering. Compos Part B 2016;92:94-132.

[18] Paunikallio T, Kasanen J, Suvanto M, Pakkanen TT. Influence of maleated polypropylene on mechanical properties of composite made of viscose fiber and polypropylene. J Appl Polym Sci 2003;87(12):1895-900.

[19] Shibata M, Oyamada S, Kobayashi Si, Yaginuma D. Mechanical properties and biodegradability of green composites based on biodegradable polyesters and lyocell fabric. J Appl Polym Sci 2004;92(6):3857-63.

[20] Paunikallio T, Suvanto M, Pakkanen T. Composition, tensile properties, and dispersion of polypropylene composites reinforced with viscose fibers. J Appl Polym Sci 2004;91(4):2676-84.

[21] Ganster J, Fink H-P. Novel cellulose fibre reinforced thermoplastic materials. Cellulose 2006;13(3):271-80.

[22] Fink HP, Ganster J. Novel Thermoplastic Composites from Commodity Polymers and Man-Made Cellulose Fibers. Macromol Symp 2006;224:107-18.

[23] Bax B, Müssig J. Impact and tensile properties of PLA/Cordenka and PLA/flax composites. Compos Sci Technol 2008;68(7):1601-7.

[24] Huber T, Pang S, Staiger MP. All-cellulose composite laminates. Compos Part A 2012;43(10):1738-45.

[25] Huber T, Bickerton S, Müssig J, Pang S, Staiger MP. Flexural and impact properties of all-cellulose composite laminates. Compos Sci Technol 2013;88:92-8.

[26] Pöllänen M, Suvanto M, Pakkanen TT. Cellulose reinforced high density polyethylene composites—Morphology, mechanical and thermal expansion properties. Compos Sci Technol 2013;76:21-8.

[27] Venkateshwaran N, Perumal AE, Arunsundaranayagam D. Fiber surface treatment and its effect on mechanical and visco-elastic behaviour of banana/epoxy composite. Mater Design 2013;47:151-9.

©2018, Elsevier. This manuscript version is made available under the CC-BY-NC-ND 4.0 license http://creativecommons.org/licenses/by-nc-nd/4.0/

[28] Zafeiropoulos N, Williams D, Baillie C, Matthews F. Engineering and characterisation of the interface in flax fibre/polypropylene composite materials. Part I. Development and investigation of surface treatments. Compos Part A 2002;33(8):1083-93.

[29] Sdrobiş A, Darie RN, Totolin M, Cazacu G, Vasile C. Low density polyethylene composites containing cellulose pulp fibers. Compos Part B 2012;43(4):1873-80.

[30] Fancey KS. Investigation into the feasibility of viscoelastically generated pre-stress in polymeric matrix composites. Mater Sci Eng A 2000;279(1):36-41.

[31] Pang JWC, Fancey KS. Analysis of the tensile behaviour of viscoelastically prestressed polymeric matrix composites. Compos Sci Technol 2008;68(7):1903-10.

[32] Pang JWC, Fancey KS. The flexural stiffness characteristics of viscoelastically prestressed polymeric matrix composites. Compos Part A 2009;40(6):784-90.

[33] Fancey KS. Viscoelastically prestressed polymeric matrix composites–Potential for useful life and impact protection. Compos Part B 2010;41(6):454-61.

[34] Fazal A, Fancey KS. Viscoelastically prestressed polymeric matrix composites–effects of test span and fibre volume fraction on Charpy impact characteristics. Compos Part B 2013;44(1):472-9.

[35] Wang B, Fancey KS. Towards optimisation of load-time conditions for producing viscoelastically prestressed polymeric matrix composites. Compos Part B 2016;87:336-42.

[36] Fancey KS, Fazal A. Prestressed polymeric matrix composites: Longevity aspects. Polym Compos 2016;37(7):2092-7.

[37] Fazal A, Fancey KS. Viscoelastically generated prestress from ultra-high molecular weight polyethylene fibres. J Mater Sci 2013;48(16):5559-70.

[38] Fazal A, Fancey KS. UHMWPE fibre-based composites: Prestress-induced enhancement of impact properties. Compos Part B 2014;66:1-6.

[39] Fancey KS. Viscoelastically prestressed polymeric matrix composites: An overview. J Reinf Plast Compos 2016;35(17):1290-301.

[40] O'Shaughnessy M. An experimental study of the creep of rayon. Text Res J 1948;18(5):263-80.

[41] Nissan A, Sternstein S. Cellulose as a viscoelastic material. Pure Appl Chem 1962;5(1-2):131-46.

[42] Yu Y, Jiang Z, Fei B, Wang G, Wang H. An improved microtensile technique for mechanical characterization of short plant fibers: a case study on bamboo fibers. J Mater Sci 2011;46(3):739-46.

[43] Guicheret-Retel V, Cisse O, Placet V, Beaugrand J, Pernes M, Boubakar ML. Creep behaviour of single hemp fibres. Part II: Influence of loading level, moisture content and moisture variation. J Mater Sci 2015;50(5):2061-72.

[44] Cisse O, Placet V, Guicheret-Retel V, Trivaudey F, Boubakar ML. Creep behaviour of single hemp fibres. Part I: viscoelastic properties and their scattering under constant climate. J Mater Sci 2015;50(4):1996-2006.

[45] Cui HX, Guan MJ, Zhu YX, Zhang ZZ. The flexural characteristics of prestressed bamboo slivers reinforced parallel strand lumber (PSL). Key Eng Mater 2012;517:96-100..

[46] Fancey KS. A Latch-Based Weibull Model for Polymeric Creep and Recovery. J Polym Eng 2001;21(6):489-510.

[47] Pang JW, Lamin BM, Fancey KS. Force measurement from viscoelastically recovering Nylon 6, 6 fibres. Mater Lett 2008;62(10):1693-6.

[48] Fancey KS. Prestressed polymeric composites produced by viscoelastically strained nylon 6, 6 fibre reinforcement. J Reinf Plast Compos 2000;19(15):1251-66.

©2018, Elsevier. This manuscript version is made available under the CC-BY-NC-ND 4.0 license http://creativecommons.org/licenses/by-nc-nd/4.0/

[49] Fancey KS. Fiber-reinforced polymeric composites with viscoelastically induced prestress. J Adv Mater 2005;37(2):21-9.

[50] ASTM D790, Standard Test Methods for Flexural Properties of Unreinforced and Reinforced Plastics and Electrical Insulating Materials. 2010.

[51] Dadashian F, Yaghoobi Z, Wilding M. Thermal behaviour of lyocell fibres. Polym Test 2005;24(8):969-77.

[52] Pang JWC, Fancey KS. An investigation into the long-term viscoelastic recovery of Nylon 6, 6 fibres through accelerated ageing. Mater Sci Eng A 2006;431(1):100-5.

[53] Fazal A. Polymer fibre composites: investigation into performance enhancement through viscoelastically generated pre-stress [PhD Thesis]: University of Hull; 2014.

[54] Wang B, Fancey KS. A bistable morphing composite using viscoelastically generated prestress. Mater Lett 2015;158:108-10.

[55] Wang B, Ge C, Fancey KS. Snap-through behaviour of a bistable structure based on viscoelastically generated prestress. Compos Part B 2017;114:23-33.

[56] Ladizesky N, Ward I. Ultra-high-modulus polyethylene fibre composites: I—The preparation and properties of conventional epoxy resin composites. Compos Sci Technol 1986;26(2):129-64.

[57] Fazal A, Fancey KS. Performance enhancement of nylon/kevlar fiber composites through viscoelastically generated pre-stress. Polym Compos 2014;35(5):931-8.

[58] Curtis PT, editor, CRAG test methods for the measurement of engineering properties of fibre reinforced plastics. Royal Aerospace Establishment Technical Report TR88012, UK, 1988, Part 3, p.21.

[59] BS EN ISO 179-1, Plastics–Determination of Charpy impact properties. 2010.

[60] Woodings C. Regenerated cellulose fibres: Woodhead Publishing; 2001.

[61] Motahhari S, Cameron J. Fibre prestressed composites: improvement of flexural properties through fibre prestressing. J Reinf Plast Compos. 1999;18(3):279-88.

[62] Manders PW, Chou T-W. Enchancement of strength in composites reinforced with previously stressed fibers. J Compos Mater. 1983;17(1):26-44.

[63] Davallo M, Pasdar H, Mohseni M. Mechanical properties of unsaturated polyester resin. Int J Chemtech Res 2010;2(4):2113-7.

[64] Mostafa NH, Ismarrubie Z, Sapuan S, Sultan M. The influence of equi-biaxially fabric prestressing on the flexural performance of woven E-glass/polyester-reinforced composites. J Compos Mater 2016;50(24):3385-93.

©2018, Elsevier. This manuscript version is made available under the CC-BY-NC-ND 4.0 license http://creativecommons.org/licenses/by-nc-nd/4.0/

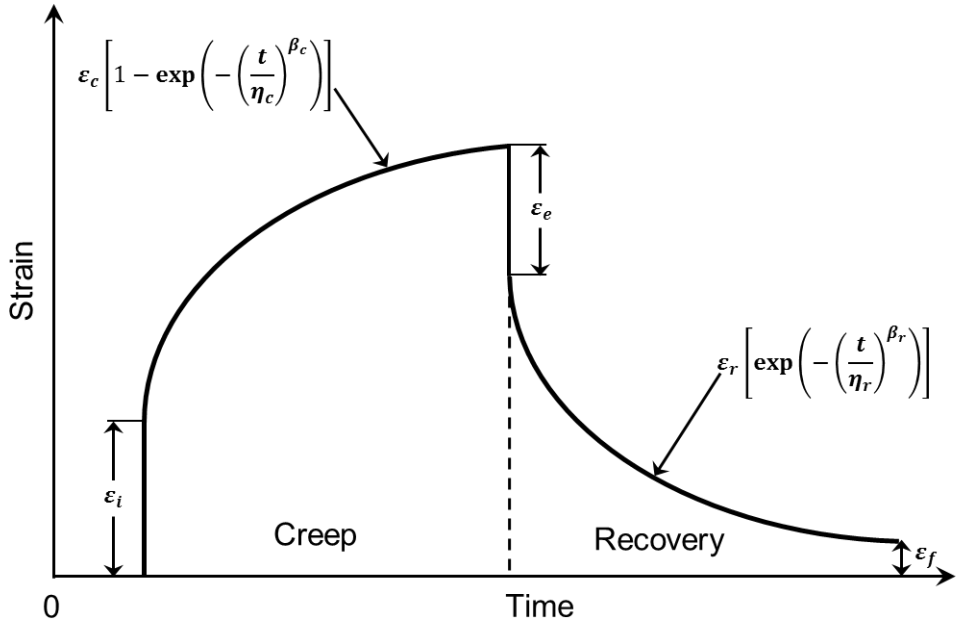

Fig. 1. Schematic of the creep-recovery cycle.

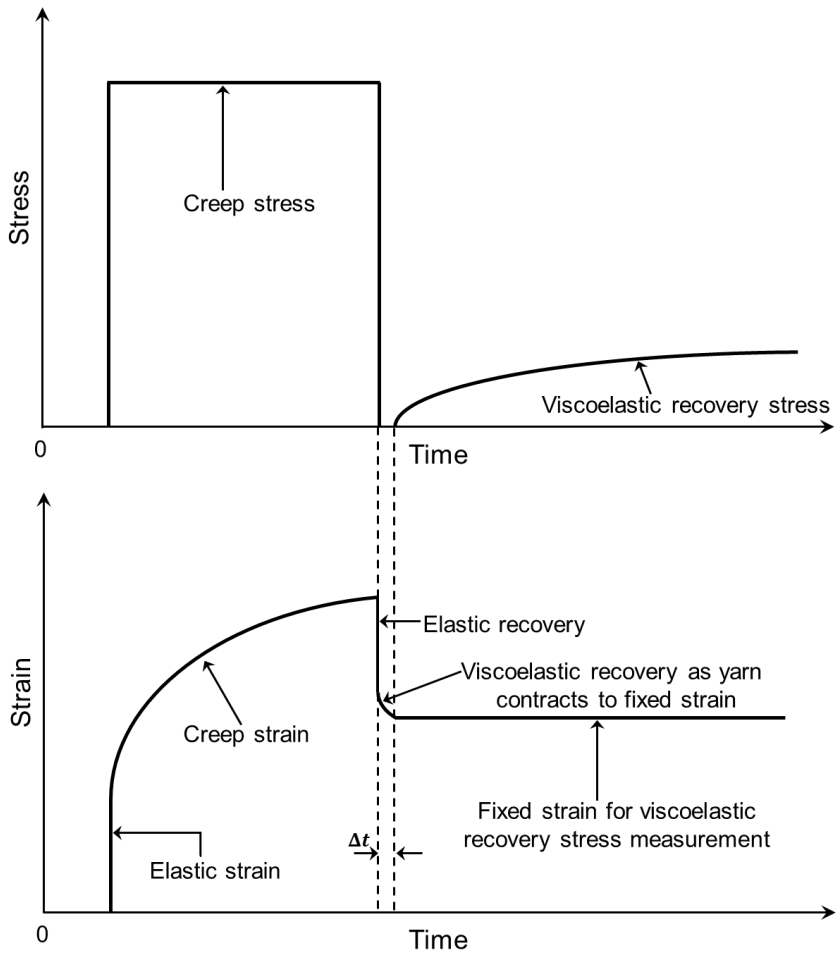

Fig. 2. The creep-recovery cycle for viscoelastic recovery stress measurement.

©2018, Elsevier. This manuscript version is made available under the CC-BY-NC-ND 4.0 license http://creativecommons.org/licenses/by-nc-nd/4.0/

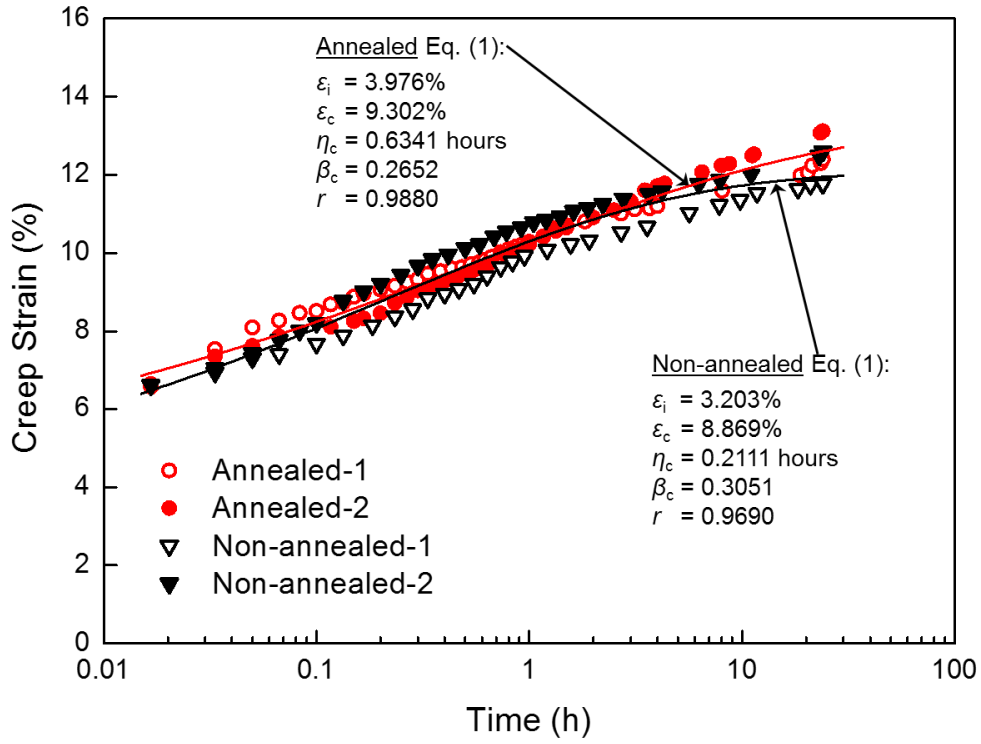

Fig. 3. Creep strain-time results for annealed and non-annealed cellulose yarns with curve-fit parameters from Eq. (1); *r* is the correlation coefficient.

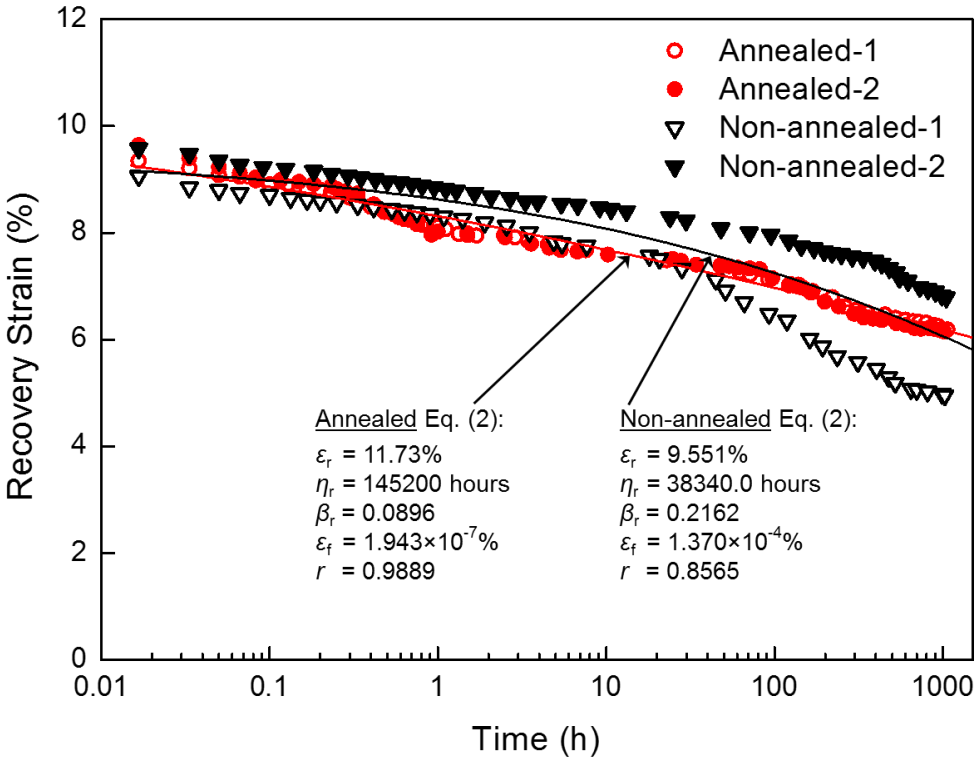

Fig. 4. Recovery strain-time results corresponding to the creep data of Fig. 3 with curve-fit parameters from Eq. (2); *r* is the correlation coefficient.

©2018, Elsevier. This manuscript version is made available under the CC-BY-NC-ND 4.0 license http://creativecommons.org/licenses/by-nc-nd/4.0/

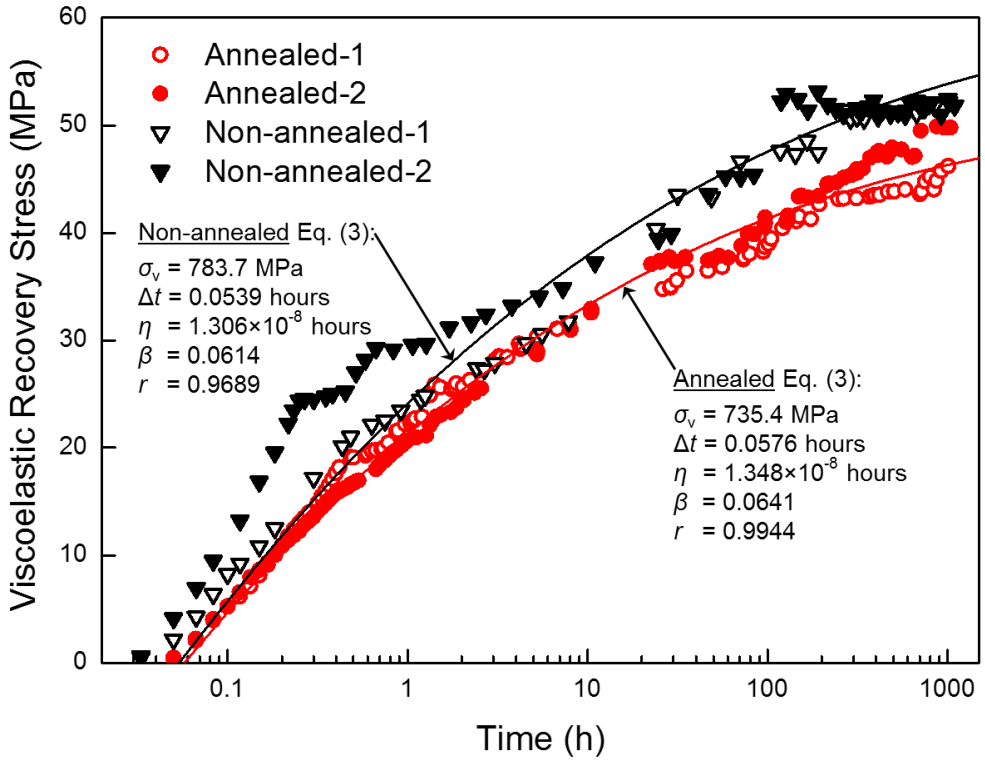

Fig. 5. Recovery stress-time results for annealed and non-annealed cellulose yarns with curve-fit parameters from Eq. (3); r is the correlation coefficient.

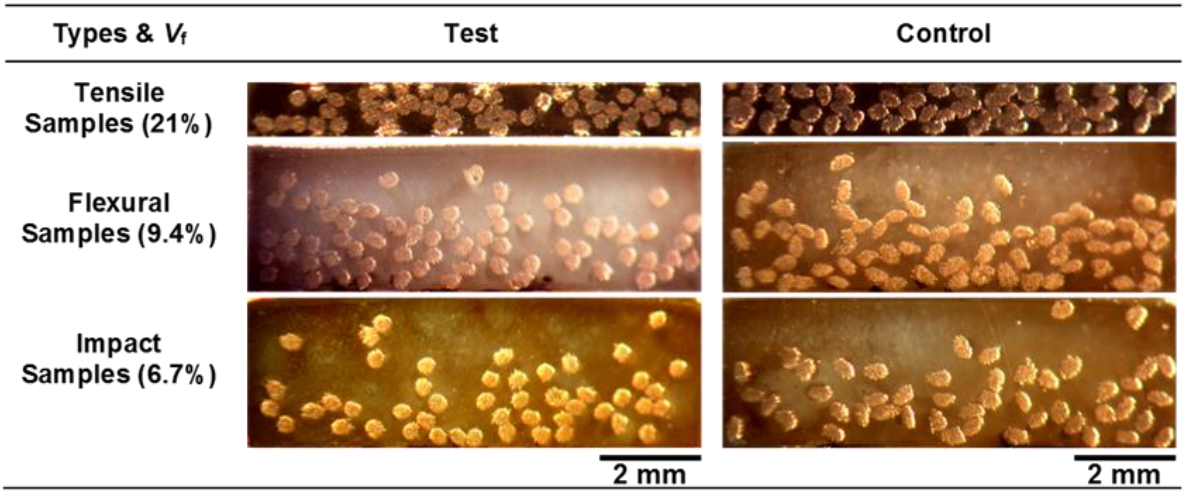

Fig. 6. Representative optical micrograph (polished) sections from all three sample types; for tensile samples, only the 21% V_f samples are shown.

©2018, Elsevier. This manuscript version is made available under the CC-BY-NC-ND 4.0 license http://creativecommons.org/licenses/by-nc-nd/4.0/

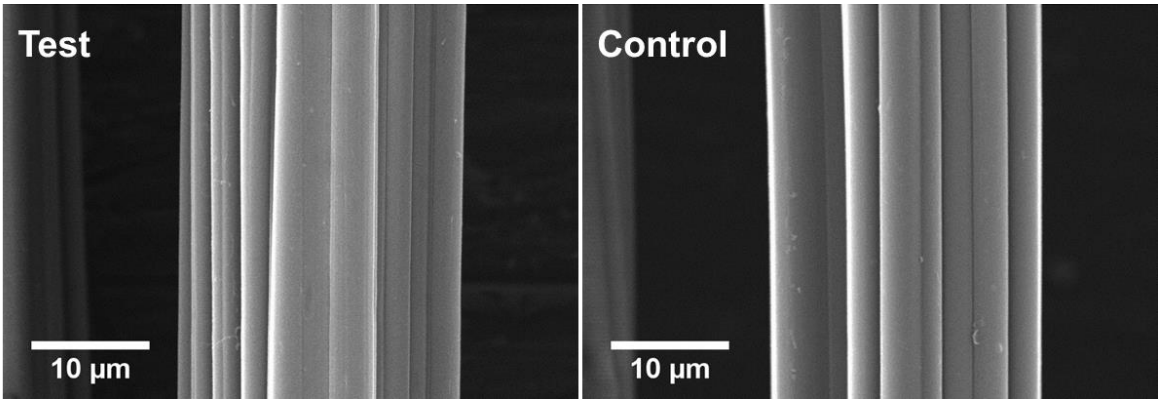

Fig. 7. SEM micrographs of test and control annealed cellulose fibres.

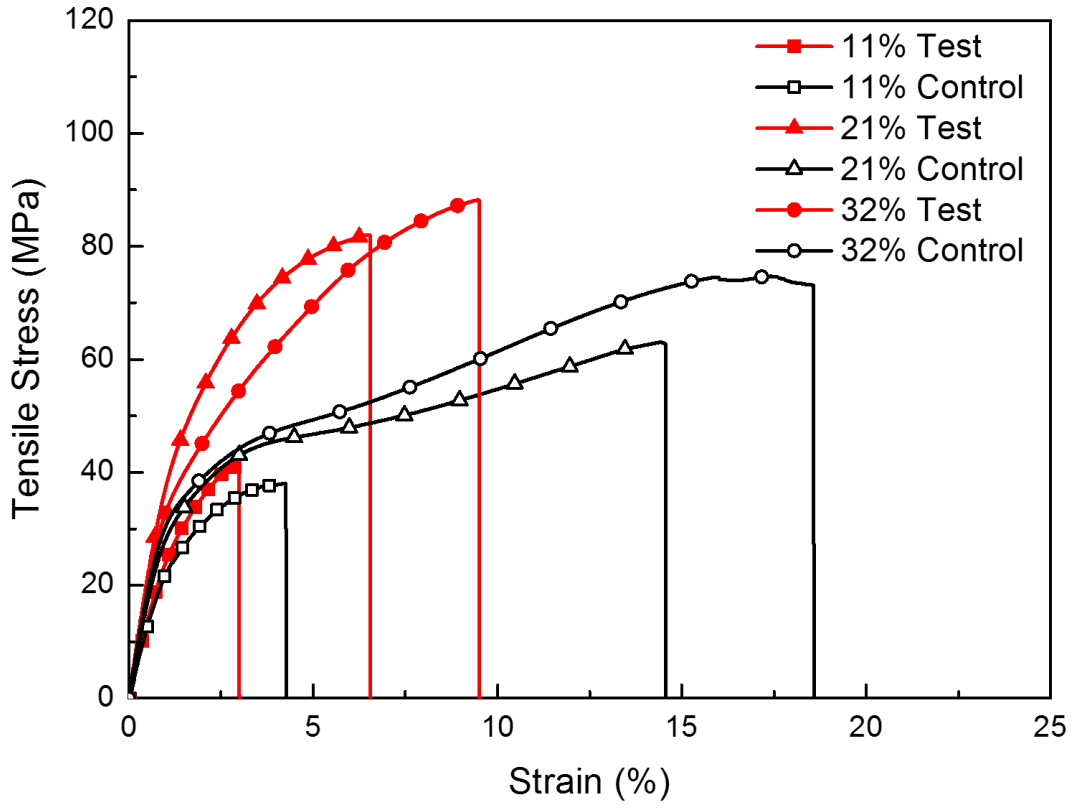

Fig. 8. Typical tensile stress-strain curves for both test and control samples at 11%, 21% and 32% V_f; the tensile modulus is measured from 0–0.33% strain.

©2018, Elsevier. This manuscript version is made available under the CC-BY-NC-ND 4.0 license http://creativecommons.org/licenses/by-nc-nd/4.0/

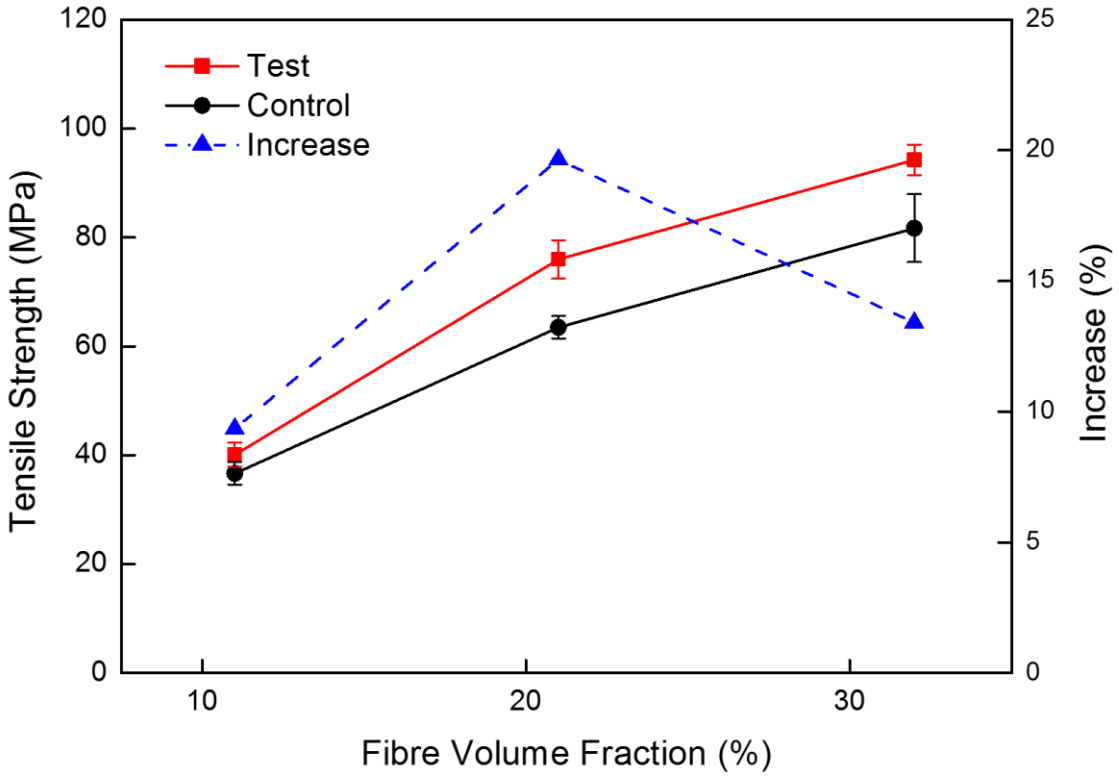

Fig. 9. Tensile strength results for both test and control samples plotted against V_f. Error bars indicate the standard error.

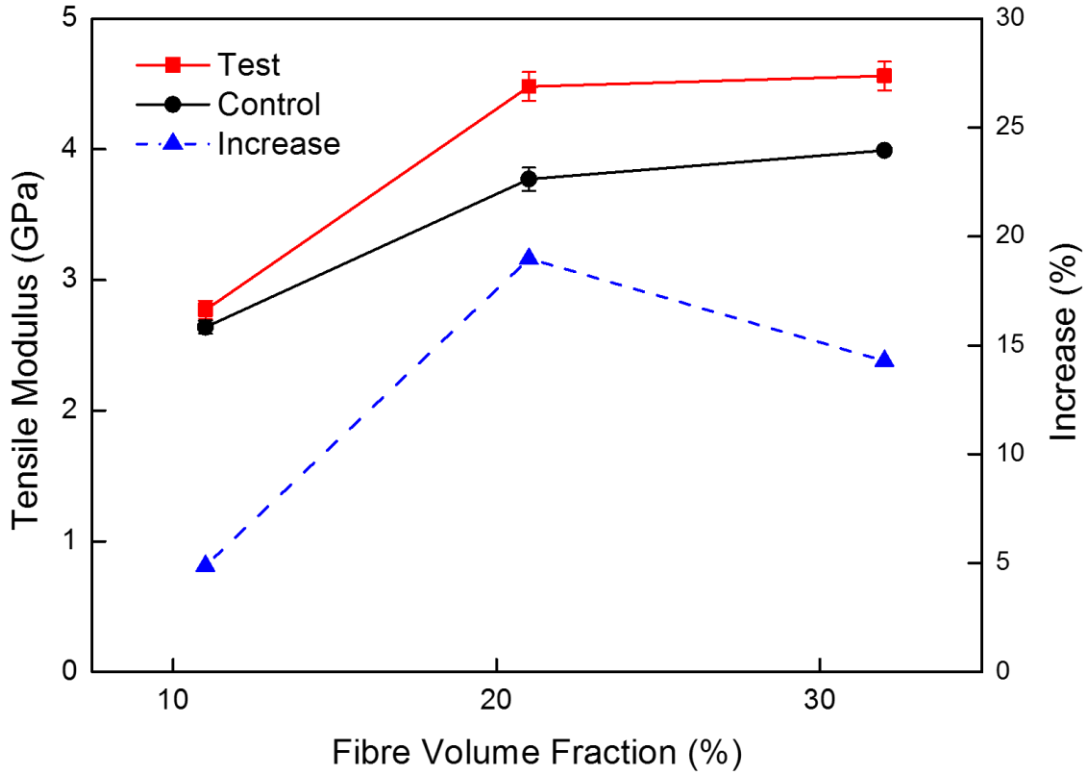

Fig. 10. Tensile modulus results for both test and control samples plotted against V_f. Error bars indicate the standard error.

©2018, Elsevier. This manuscript version is made available under the CC-BY-NC-ND 4.0 license http://creativecommons.org/licenses/by-nc-nd/4.0/

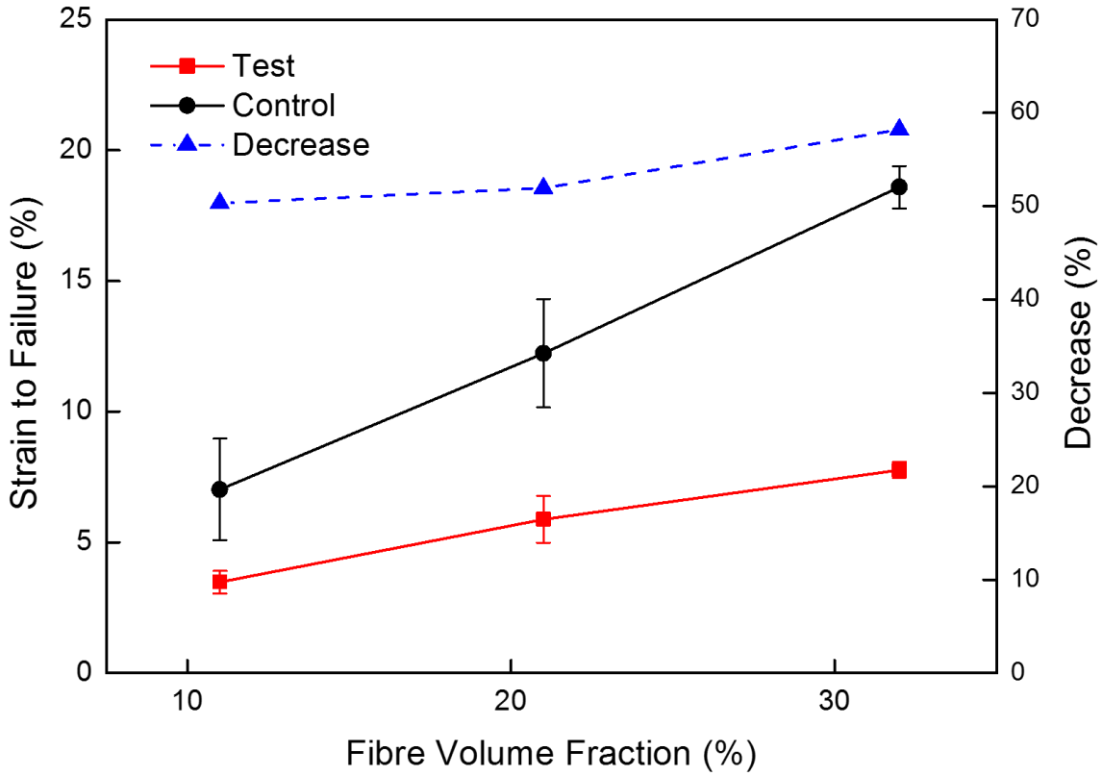

Fig. 11. Strain to failure results for both test and control samples plotted against V_f. Error bars indicate the standard error.

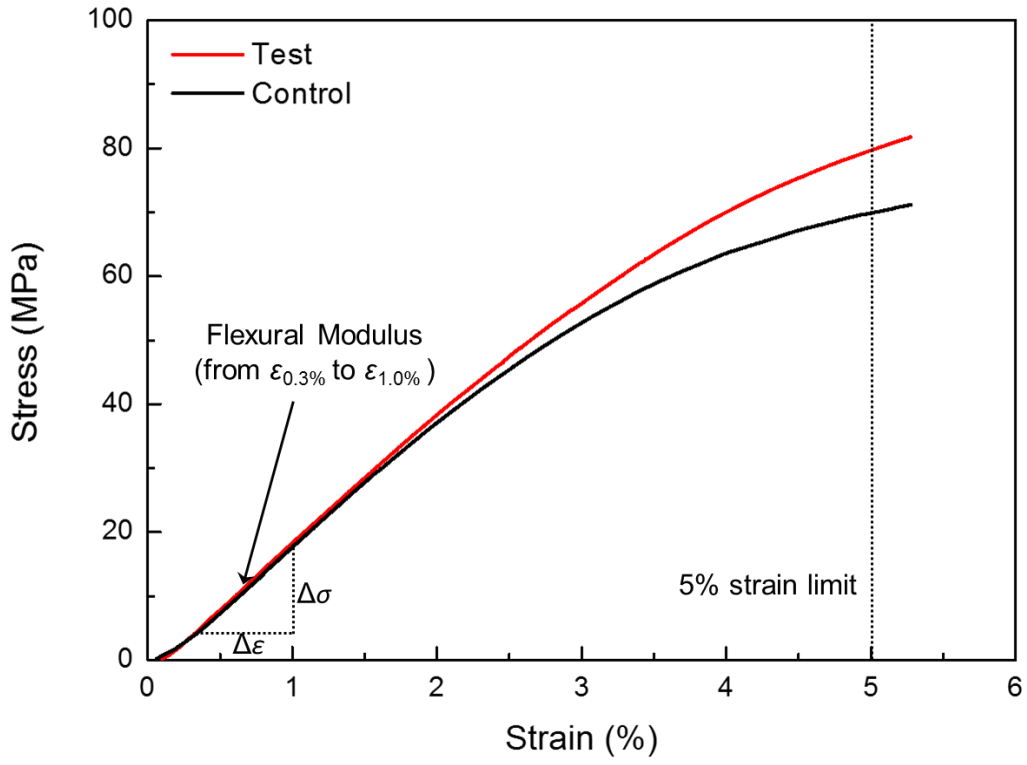

Fig. 12. Typical flexural stress-strain curves for both test and control samples, the flexural modulus is measured from 0.3–1.0% strain.

©2018, Elsevier. This manuscript version is made available under the CC-BY-NC-ND 4.0 license http://creativecommons.org/licenses/by-nc-nd/4.0/

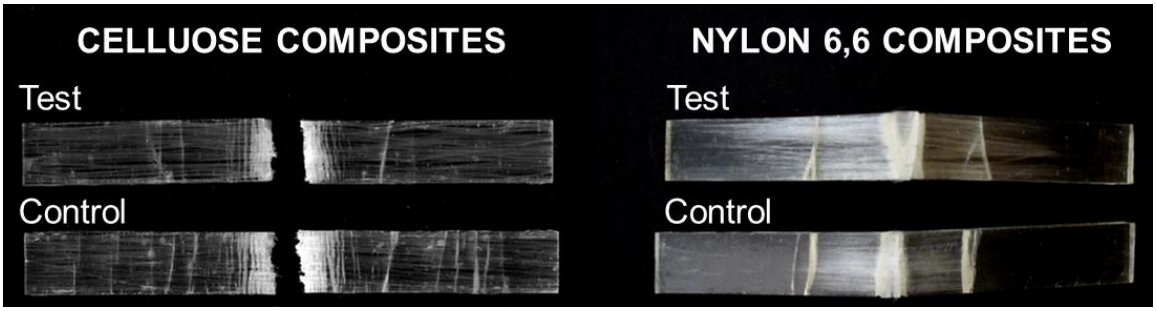

Fig. 13. Comparison of fracture characteristics between cellulose fibre and nylon 6,6 fibre-based composites following Charpy impact tests. Note that the lighter regions in the vicinity of the cellulose composite fracture represent high-density vertical cracking, while the lighter regions on the nylon 6,6 composites principally represent fibre-matrix debonding.

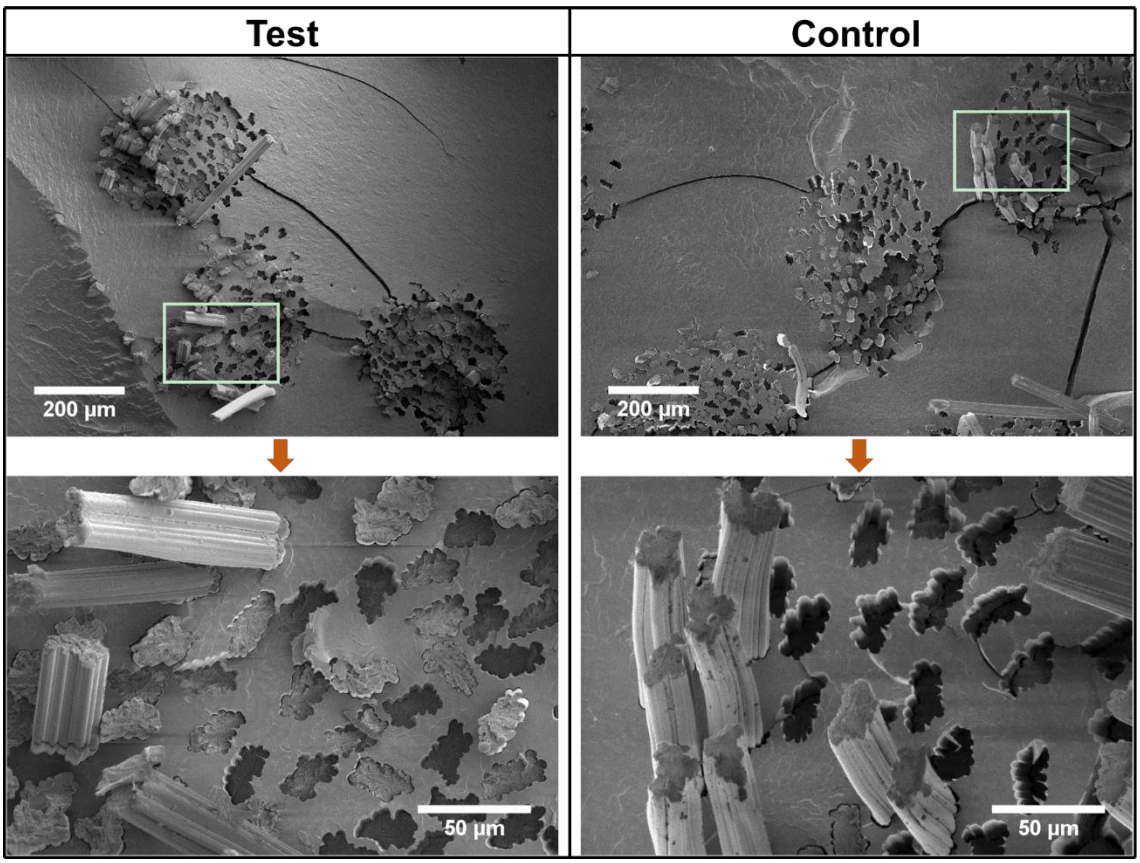

Fig. 14. SEM micrographs of typical fracture sections for both test and control samples after Charpy impact tests at two levels of magnification.

©2018, Elsevier. This manuscript version is made available under the CC-BY-NC-ND 4.0 license http://creativecommons.org/licenses/by-nc-nd/4.0/